The dynamics analysis of the inertial vibrating screen with two shafts

Yang LIU*, Juqian ZHANG, Yanzhen LI, Tuo SHI, Bangchun WEN

College of Mechanical Engineering and Automation, Northeastern University, Shenyang City, 110819, China

Abstract
In view of the problems of the balanced elliptical shale shaker in practical application. We simplified the model, established the dynamic equation for it and derived the expressions of the amplitude and phase difference angle of the inertial vibrating screen with two shafts. The key position of the amplitude, velocity, acceleration and other important data are obtained by using the B&K test and analysis system. We got modal results by comprehensive simulation modeling. We put forward the dynamic optimized design scheme of the inertial vibrating screen with two shafts and pro-vided a theoretical basis for the improvement of shale shaker performance.
Key words: BALANCED ELLIPTICAL SHALE SHAKER, DYNAMIC EQUATIONS, AMPLITUDE, PHASE DIFFERENCE ANGLE, INERTIAL VIBRATING SCREEN WITH TWO SHAFTS

1. Introduction

The performance of drilling fluid and the degree of purification directly influences drilling speed, well quality, cementing quality and the occurrence of down hole accident. Along with the popularization and application of high pressure injection, shielding temporary plugging, horizontal well and under-balanced drilling, it puts forward higher requirements on the performance and the degree of purification of the drilling fluid. It has been paid widespread attention to studying solid control equipment. The first basic screening equipment of the drilling fluid solid-control called drilling fluid shale shaker has got rapid development. It has a very important significance to improve the theoretical research and the level of the design of drilling fluid shale shaker so as to reduce the cost of drilling and improve the overall economic benefits of drilling.

2. Dynamical equation

The type of balanced elliptical shale shaker is two shafts vibrating screen with forced synchronization and inertia. The screen box is at the translational state. The difference from non-balanced elliptical shale shaker lies in the similarity between the long axis and short axis of elliptic motion locus on the screen box. Fig.1 is the schematic diagram of the motion form for elliptical shale shaker. The magnitude and direction of the circular projection angle is completely consistent. Elliptical shale shaker integrated the advantages of linear shaker and round-shaped shaker. Balanced elliptical shale shaker can be simplified as shown in Fig. 2 [1-3].

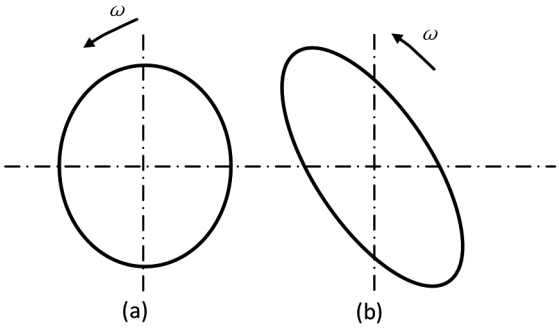

Figure 1. The motion trajectories figure of elliptical vibrating screen box

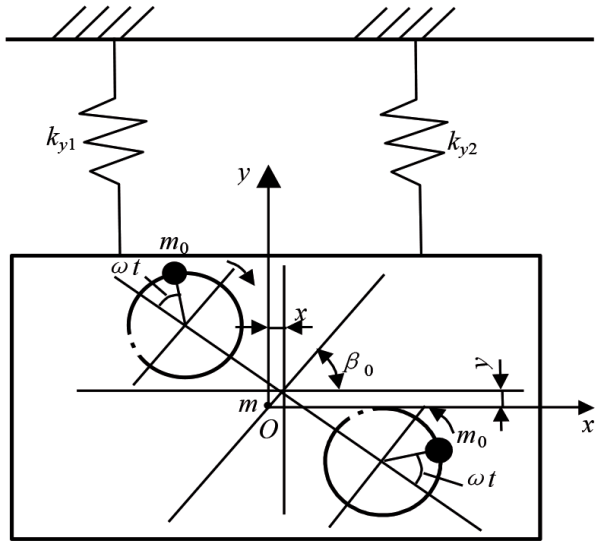

Figure 2. The force diagram of inertial screen with two shafts

In addition to the inertia force of the absolute motion produced by the eccentric block, there are inertia force $F_{my} = -m\ddot{y}$, $F_{mx} = -m\ddot{x}$, damping force $F_{fy} = -f\dot{y}$, $F_{fy} = -f\dot{x}$ and elastic force $F_{ky} = -ky$, $F_{kx} = 0$ of the vibration body. According to the dynamic and static method in theoretical mechanics, all these force sum to zero.

Y direction

$$-m\ddot{y} - f\dot{y} - ky - 2m_0(\ddot{y} - \omega^2 r\sin\beta_0\sin\omega t) = 0$$

X direction

$$-m\ddot{x} - f\dot{x} - 2m_0(\ddot{x} - \omega^2 r\cos\beta_0\sin\omega t) = 0 \qquad (1)$$

In which, $m = m_p + K_m m_m$.

m_p – the actual quality of vibration body.

K_m – material combination coefficient.

m_m – material quality.

f – equivalent drag coefficient.

k – the stiffness in the centering direction of the isolation springs, $k = k_{y1} + k_{y2}$.

y, $\dot{y}$, $\ddot{y}$ and x, $\dot{x}$, $\ddot{x}$ – displacement, velocity and acceleration in Y and X direction of the vibration body.

Transpose the upper formulae, we can obtain the formulae as following:

$$\begin{cases}(m+2m_0)\ddot{y} + f\dot{y} + ky = 2m_0\omega^2 r\sin\beta_0\sin\omega t \\ (m+2m_0)\ddot{x} + f\dot{x} = 2m_0\omega^2 r\cos\beta_0\sin\omega t\end{cases} \qquad (2)$$

The upper formulae is the differential equation of the two shafts vibrating screen with inertia along the Y and X direction .We will seek the vibration equation below.

Set the displacement in the x direction and y direction as follows:

$$y = \lambda_y\sin(\omega t - a_y) \qquad x = \lambda_x\sin(\omega t - a_x) \qquad (3)$$

In which, λ_y, λ_x – the amplitude in Y and X direction.

a_y, a_x – the phase difference angle caused by the exciting force in Y and X direction relative to the displacement.

Velocity and acceleration are given as follows:

$$\begin{cases}\dot{y} = \lambda_y\omega\cos(\omega t - a_y) \\ \ddot{y} = -\lambda_y\omega^2\sin(\omega t - a_y) \\ \dot{x} = \lambda_x\omega\cos(\omega t - a_x) \\ \ddot{x} = -\lambda_x\omega^2\sin(\omega t - a_x)\end{cases} \qquad (4)$$

Take the generation of the velocity and acceleration into the type (2) by adopting the same method with single shaft inertia vibrating screen machine. It can be obtained as follows:

$$\begin{cases}-(m+2m_0)\omega^2\lambda_y + k\lambda_y = 2m_0\omega^2 r\sin\beta_0\cos a_y \\ f\omega\lambda_y = 2m_0\omega^2 r\sin\beta_0\sin a_y \\ -(m+2m_0)\omega^2\lambda_x = 2m_0\omega^2 r\cos\beta_0\cos a_x \\ f\omega\lambda_x = 2m_0\omega^2 r\cos\beta_0\sin a_x\end{cases} \qquad (5)$$

According to the upper formula, we can calculate the amplitude of the biaxial inertia vibrating machine in Y direction and X direction λ_y, λ_x and the phase difference angle a_y, a_x as follows:

$$\begin{cases}\lambda_y = \dfrac{2m_0\omega^2 r\sin\beta_0\cos a_y}{k-(m+2m_0)\omega^2} = -\dfrac{2m_0 r\sin\beta_0\cos\alpha_y}{m'_y} \\ \lambda_x = \dfrac{2m_0 r\cos\beta_0\cos a_x}{-(m+2m_0)} = -\dfrac{2m_0 r\cos\beta_0\cos a_x}{m'_x} \\ a_y = \arctan\dfrac{f\omega}{k-(m+2m_0)\omega^2} = \arctan\dfrac{-f}{m'_y\omega} \\ a_x = \arctan\dfrac{-f}{(m+2m_0)\omega} = \arctan\dfrac{-f}{m'_x\omega}\end{cases} \qquad (6)$$

In which, $m'_y = m + 2m_0 - \dfrac{k}{\omega^2}$, $m'_x = m + 2m_0$.

m'_y, m'_x –computational quality in Y and X direction.

3. Actual working condition analysis

As is shown in Figure 3, a certain type of drilling fluid shale shaker belongs to this type. It has good screening effect, large processing capacity. It is a more advanced shale shaker. But its high manufacturing precision and high on-site maintenance requirements affect its popularization and application [4-7].

The overflow of drilling fluid and frequently replaced screen always occurred in the use process according to the user, which seriously affected the nor-

Figure 3. Drilling fluid shale shaker

mal production work and caused a time delay. Based on the above problems appeared in use process, quality inspection and test is of great significance for the shale shaker. Test method uses the combination of visual inspection and instrument testing. Instrument testing uses B&K test, which is shown in figure 4.

Figure 4. Measurement and analysis system

3.1. Experimental test

3.1.1. Visual inspection result (normal operation condition)

Vibrating direction angle: 45°.

Leaning angle of screen: 3.5°.

Amplitude in direction of vibration (double-amplitude): about 6.0 mm.

Amplitude in vertical direction of vibration: 1.0 mm (double).

3.1.2. Test results

The maximum acceleration of horizontal direction of the vibration in the position of the centric: 71.9 m/s^2. The maximum acceleration of vertical direction of the vibration: 19.4 m/s^2. Synthesis of horizontal direction: 71.9×cos45+19.4×sin45°=64.6 m/s^2. Synthesis of vertical direction: 71.9×sin45+19.4×cos45°= = 64.6 m/s^2. Accelerations of other position are shown in figure 5~7.

Vibration frequency is 24 Hz shown in figure 7, 24×2 =150.72 rad/s.

It can be shown that vibration frequency is 24 Hz in figure 7, 24×2 =150.72 rad/s.

Amplitude can be obtained by $A \times \omega^2 = a$ as follows:

$$A_y = a_y / \omega^2 = 71.9/150.72^2 = 0.00317\text{m} = 3.17\text{mm}$$

$$A_x = a_x / \omega^2 = 19.4/150.72^2 = 0.00085\text{m} = 0.85\text{mm}$$

In horizontal direction:

3.17×cos45°+0.85×sin45°=2.84 mm

In vertical direction:

3.17×sin45°+0.85×cos45°=2.84 mm.

It can be seen that visual inspection and test results are basically consistent according to the above data. Due to the vibrating direction angle's change between 40°, 45°and 50°, the component force of the horizontal and vertical directions are different. The more component force in vertical direction, the more permeability, and the more component force in horizontal direction, and the more transmission rate [8].

Therefore, we should increase the amplitude in the horizontal direction as well as keep the vertical amplitude unchanged (even more) so as to meet the requirements of a large number of processing drilling fluid. Fig.5 is the maximum amplitude of the vibration acceleration of 1st test point, x_max=19.4 m/s^2, y_max= 71.91 m/s^2. Fig.6 is the maximum amplitude of the vibration acceleration of 2nd test point, x_max = 22.0 m/s^2, y_max=69.9 m/s^2. Fig.7 is the spectrum in X axis for 1st test point. Vibration energy is concentrated on 24Hz.

3.2. Modal calculation

The reinforcement plate frame and the layout of the square beam and circle beam will affect the natural frequency and the corresponding vibration mode [9-10]. So it is necessary to compute the natural frequency of the screen body in order to determine whether the screen body in working condition is of possibility of a resonance. We used finite element software ANSYS for modal analysis in the case, added constraint to nodes in the spring, extracted the modal using block lanczos and output the first six natural frequencies of the screen frame by the general postprocessor (POST1) [11-13].

The first order vibration mode for the vibrating screen body is at about 50 Hz. The second to the sixth order vibration mode focus on about 60 Hz. It can be seen that the vibration displacement in the middle of the vibration screen is large. So we should pay attention to the protection of the screen body and the screen in the vibrating screen work.

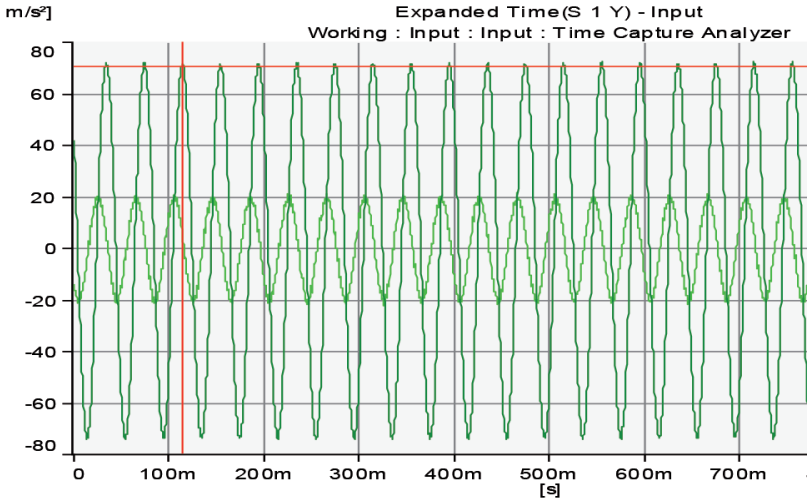

Figure 5. Vibration acceleration of the 1st test point

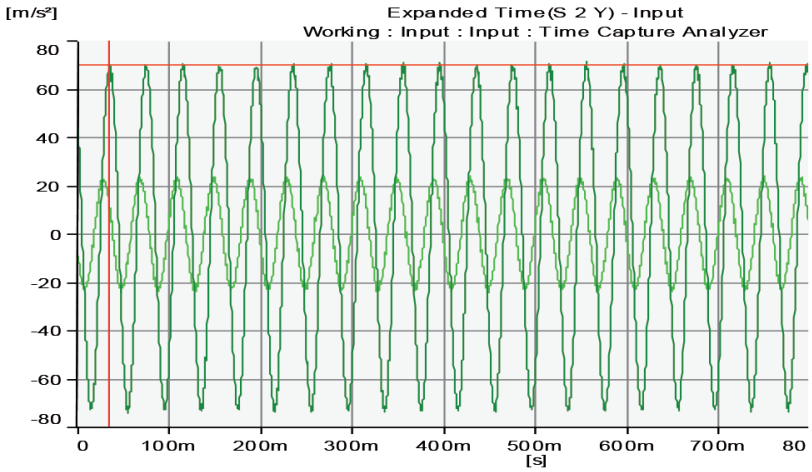

Figure 6. Vibration acceleration of the 2nd test point

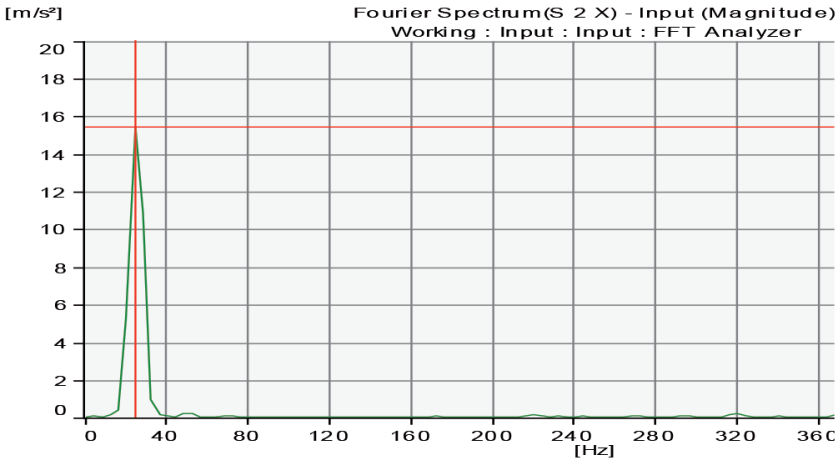

Figure 7. Spectrum of the 1st test point in X axis

Table 1. The result of calculation for 1st ~6th natural frequency of body

Order	1	2	3	4	5	6
Frequency (Hz)	49.046	59.322	59.877	60.613	61.288	61.814

Conclusions

We can obtain the dynamic optimized design scheme of the inertial vibrating screen with two shafts through the test and simulation above as well as the further analysis of the test results.

(1) To adjust the direction angle of vibration

It was 40 degrees; now tend to be 30 degrees.

Objective: to accelerate the transportation speed of the materiel on screen (sand, stone).

1) The vibrating direction angle is adjusted to 30 degrees in the view of the processing point. Material movement speed is proportional to vibration intensity as well as the cosine of vibrating direction angle. In certain vibration intensity, material movement speeds up after vibrating direction angle gets down so as to adapt to deal with a large number of drilling fluid when the drilling depth is 1000 meters. If the decrease of the vibrating direction angle still can not meet the processing requirements, the angle should be turned up to make sure the mud does not leak.

2) In view of mud and medium screening, acceleration of material movement leads to the reduction of the material layer on the screen as well as the reduction of the leaking screen's resistance of mud and medium in the condition of a certain capacity. Therefore, it is helpful to improve sieve mesh number in order to enhance the screening effect.

(2) To improve the outlet structure and heighten the height of side plate

Outlet structure must be improved for the original screen box. Keep the angle of the upper material discharge port with a flat screen surface so that the effective length of the screen surface increases. Then the possibility of the appearance of grouting off target reduces. And heighten the height of side plate to make the mud not burst out in the working process. The dip of the screen surface is generally 3 to 5 degrees interval which can ensure normal material conveying on the screen. This scheme still uses 3 degrees as same as the original screen angle. It is viable to increase the angle and sacrifice the screening effect in order to grouting off target prevention in the large amount of material treatment.

(3) To improve the fixing method for the motor bolt

Motor support plate and the motor support contact surface must be refined to meet the requirements of flatness criteria so as to ensure that the four fixing bolts are at the same stress. Installation of the motor support plate and motor uses the combined installation of bolts and dowel pin. We also use lock bolt. A dowel pin bears exciting force in the shear direction and a bolt bears tension only so as to ensure the safety of mounting of motor.

(4) To add strengthening tendon-plate

Improve the structure of stiffener and prevent cracking and deformation in side plate of the screen box in order to improve the strength and service life of the screen box.

(5) To adjust the position of the installation for the beam of the vibration motor

Taking the screen box structure and vibration motor adjustment into account, the position of the installation beam of the vibration motor should be adjusted. Namely the distance between the adjusted vibrating screen and the centric along the horizontal direction remains close to the distance of the front and back spring support. It is fit to the demand that the position of the isolation spring of the original screen keeps unchanged so as to ensure the screen body is mounted on the base without changing the machine base. We also reconfigured metal spiral isolation spring.

Acknowledgements

This work was financially supported by the National Natural Science Foundation of China for Young Scientists (Grant No.51105065), Exploration-oriented Key Scientific and Technological Innovation Project from Ministry of Education of China (Grant No.N140304005), National Science Foundation for Postdoctoral Scientists of China (2014M551105, 2015T80269).

References

1. Z. Yuemin, L. Chusheng. Dynamic design theory and application of large vibrating screen. Procedia Earth and Planetary Science, 2009, vol. 1, p.p. 776-778.
2. R.T. Fowler, S.C. Lim. The influence of various factors upon the effectiveness of separation of a finely divided solid by a vibrating screen. Chemical Engineering Science, 1959, vol. 10, p.p. 163-170.
3. H. Xiaomei, L. Chu-sheng. Dynamics and screening characteristics of a vibrating screen with variable elliptical trace (In Chinese). Mining Science and Technology, 2009, vol. 19, p.p. 508-513.
4. S. Yan, J. Xiaohong, S. Juan, Z. Jianxun. Dynamic analysis of a chaotic vibrating screen (In Chinese). Procedia Earth and Planetary Science, 2014, vol. 6, p.p. 1525-1531.

5. L. Xingyang, C. Guo. The dynamic analysis of rotor/ball bearings systems misalignment-rubbing coupling faults (In Chinese). Aircraft Design, 2009, vol. 29, p.p. 71-80.
6. H. Zhiwei, Z. Jianzhong, Z. Yongchuan. Dynamic analysis on hydraulic generator rotors with coupling faults of misalignment and rub-impact (In Chinese). Proceedings of the CSEE, Beijing, 2010, pp. 88-93.
7. H. Qingkai, Y. Tao, W. Deyou. Nonlinear Vibration Analysis and Diagnosis Methods of Fault Rotor System (In Chinese), Science Press, 2010, 321 p.
8. W. Bangchun, W. XingHong, D. Qian. The Nonlinear Dynamics Theory and Experiment of Fault Rotating Machinery, Science Press, 2004, 112 p.
9. M.A. Bradford, N.A. Yazdi. Newmark-based method for the stability of columns. Elsevier Science Ltd, 1999, vol. 71, p.p. 689-700.
10. Z. Junhong, M. Liang, L. Jiewei. Dynamic analysis of flexible rotor-ball bearings system with unbalance-misalignment-rubbing coupling faults. Trans Tech Publications, 2012, vol. 105-107, p.p. 448-453.
11. L. Changli, X. Pengru, Z. Shaoping. Dynamics Characteristics of Rotor with Breathing Crack Using Finite Element Method (In Chinese), Journal of Vibration, Measurement & Diagnosis, 2011, vol. 31, p.p. 185-189.
12. W. Yan, M. Jisheng, Z. Haiqi. Dynamic Characteristics Analysis of Gear-Bearing System with Flexible Rotor (In Chinese), Journal of Vibration, Measurement & Diagnosis, 2012, vol. 32, p.p. 51-55.
13. V. Barzdaitis, M. Bogdevicius, R. Didziokas. Diagnostics procedure for identification of rubs in rotor bearings. Journal of Vibroengineering, 2010, vol. 12, p.p. 552-565.